RAD51C deficiency in mice results in early prophase I arrest in males and sister chromatid separation at metaphase II in females

Sergey Kuznetsov,[1] Manuela Pellegrini,[2] Kristy Shuda,[3] Oscar Fernandez-Capetillo,[2] Yilun Liu,[4] Betty K. Martin,[1] Sandra Burkett,[1] Eileen Southon,[1] Debananda Pati,[5] Lino Tessarollo,[1] Stephen C. West,[4] Peter J. Donovan,[6] Andre Nussenzweig,[2] and Shyam K. Sharan[1]

[1]Mouse Cancer Genetics Program, Center for Cancer Research, National Cancer Institute at Frederick, Frederick, MD 21702
[2]Experimental Immunology Branch, National Cancer Institute, Bethesda, MD 20892
[3]Kimmel Cancer Center, Thomas Jefferson University, Philadelphia, PA 19107
[4]Cancer Research UK, London Research Institute, Clare Hall Laboratories, South Mimms, Herts EN6 3LD, England, UK
[5]Department of Pediatrics, Texas Children's Cancer Center, Baylor College of Medicine, Houston, TX 77030
[6]Institute for Cell Engineering, Johns Hopkins University, Baltimore, MD 21205

RAD51C is a member of the RecA/RAD51 protein family, which is known to play an important role in DNA repair by homologous recombination. In mice, it is essential for viability. Therefore, we have generated a hypomorphic allele of *Rad51c* in addition to a null allele. A subset of mice expressing the hypomorphic allele is infertile. This infertility is caused by sexually dimorphic defects in meiotic recombination, revealing its two distinct functions. Spermatocytes undergo a developmental arrest during the early stages of meiotic prophase I, providing evidence for the role of RAD51C in early stages of RAD51-mediated recombination. In contrast, oocytes can progress normally to metaphase I after superovulation but display precocious separation of sister chromatids, aneuploidy, and broken chromosomes at metaphase II. These defects suggest a possible late role of RAD51C in meiotic recombination. Based on the marked reduction in Holliday junction (HJ) resolution activity in *Rad51c*-null mouse embryonic fibroblasts, we propose that this late function may be associated with HJ resolution.

Introduction

Bacterial RecA and its yeast orthologue RAD51 are the founding members of the RecA/RAD51 protein family, which plays a crucial role in DNA repair by homologous recombination (for review see Kawabata et al., 2005). After DNA ends are resected at the site of a DNA break, these proteins form a nucleoprotein filament on the single-stranded DNA and catalyze a strand invasion and strand exchange reaction with a homologous region on another DNA molecule to ensure faithful DNA repair. In addition to RAD51, a few other RAD51-like proteins were found in eukaryotes, with their number increasing from three in budding yeast (Rad55, Rad57, and Dmc1) to six in most of the higher eukaryotes (RAD51B, RAD51C, RAD51D, XRCC2, XRCC3, and DMC1; Dosanjh et al., 1998). These proteins have 20–30% amino acid sequence similarity and share common functional domains (Miller et al., 2004). The core C-terminal domain contains two functionally important ATP-binding Walker A and B motifs and is linked to a small globular N-terminal domain via a linker region that is important for protein–protein interactions.

Except for DMC1, a meiosis-specific protein with functions overlapping those of RAD51 (Bishop et al., 1992), the other five paralogues are auxiliary to RAD51. In yeast, the purified Rad55/Rad57 heterodimer functions as a mediator of Rad51, enabling it to nucleate on single-stranded DNA in the presence of replication protein A (RPA; Sung, 1997). Chicken DT40

M. Pellegrini, K. Shuda, and O. Fernandez-Capetillo contributed equally to this paper.

Correspondence to Shyam K. Sharan: ssharan@mail.ncifcrf.gov

O. Fernandez-Capetillo's present address is Spanish National Cancer Center, 28029 Madrid, Spain.

P.J. Donovan's present address is Stem Cell Program and Dept. of Biological Chemistry and Developmental and Cell Biology, University of California, Irvine, Irvine, CA 92697.

Abbreviations used in this paper: DSB, double strand break; GV, germinal vesicle; hCG, human chorionic gonadotropin; HJ, Holliday junction; MEF, mouse embryonic fibroblast; neo, neomycin; PGK, phosphoglycerate kinase; PMS, pregnant mare serum; PSSC, precocious separation of sister chromatids; RPA, replication protein A.

The online version of this article contains supplemental material.

The Journal of Cell Biology, Vol. 176, No. 5, February 26, 2007 581–592
http://www.jcb.org/cgi/doi/10.1083/jcb.200608130

cells and hamster cell lines deficient in any one of the five RAD51-like proteins are extremely sensitive to DNA damage caused by DNA cross-linking agents and the topoisomerase-I inhibitor camptothecin (Yonetani et al., 2005). In such cells, RAD51 foci formation after DNA damage is attenuated, and the frequency of homologous recombination is reduced (Lio et al., 2004). RAD51C and XRCC3 directly interact with RAD51, and RAD51C has been shown to stabilize RAD51 after DNA damage by protecting it from ubiquitin-mediated degradation (Bennett and Knight, 2005).

These proteins interact with one another and form multiple protein complexes (Masson et al., 2001; Sigurdsson et al., 2001). Two stable complexes have been biochemically purified. One includes RAD51B, RAD51C, RAD51D, and XRCC2 (BCDX2 complex), and the other contains RAD51C and XRCC3 (CX3 complex). The functional relevance of these complexes is supported by studies of double mutants in DT40 cells, in which two mutations in different complexes as opposed to mutations in the same complex had an additive effect on sensitivity to camptothecin (Yonetani et al., 2005).

Despite all of the aforementioned similarities and a general understanding that all RAD51 paralogues are involved in the homologous recombination process, little is known about the specific roles played by any of them. However, each of these proteins is believed to have a nonredundant function, as the loss of any of these genes cannot be compensated for by the overexpression of other family members (Takata et al., 2001). Mutations in these genes have an unequal impact on drug sensitivity in DT40 cells (Yonetani et al., 2005). Although mice that are null for any of the paralogues are embryonic lethal, they vary in the severity of the phenotype (Shu et al., 1999; Deans et al., 2000; Pittman and Schimenti, 2000). In *Arabidopsis*, *Rad51c* and *Xrcc3* mutants are sterile, whereas other mutants are fertile (Bleuyard et al., 2005). One family member, RAD51D, has been specifically linked to telomere maintenance (Tarsounas et al., 2004).

Although all RAD51 paralogues are implicated in RAD51 foci formation, it is unclear how this function is shared between different paralogues and their complexes (Yonetani et al., 2005). RAD51C is part of both BCDX2 and CX3 complexes and, therefore, is believed to play a central role. Being part of two different protein complexes, RAD51C may also have several distinct functions. On one hand, it is involved in the early steps of recombination associated with RAD51. On the other hand, it may also be involved in late steps of homologous recombination, as RAD51C, together with XRCC3, was purified from HeLa cells as part of a small protein complex possessing a Holliday junction (HJ) resolvase activity (Liu et al., 2004). RAD51C is an essential part of this complex because the resolvase activity was lost upon depletion of RAD51C from the fraction or when protein extracts from hamster cells lacking functional *Rad51c* were tested. However, the role of RAD51C as a resolvase remains controversial. RAD51C lacks an endonuclease domain, and efforts to demonstrate resolvase activity for the recombinant RAD51C protein have not been successful so far. Also, there is no in vivo evidence supporting this late role of RAD51C in recombination.

In this study, we report the generation of a viable mouse model carrying a hypomorphic allele of *Rad51c*, which enabled us to overcome the early embryonic lethality of a null allele and demonstrate the role of RAD51C in meiotic recombination. We demonstrate that RAD51C is involved in the recruitment of RAD51 at early stages of homologous recombination in spermatocytes. In oocytes, we describe a defect in sister chromatid cohesion at metaphase II. We speculate that RAD51C may also be required at late steps of homologous recombination.

Results

Generation of a hypomorphic allele of *Rad51c*

The mouse *Rad51c* gene consists of eight exons and encodes a 366–amino acid protein (Leasure et al., 2001). Exons 2 and 3

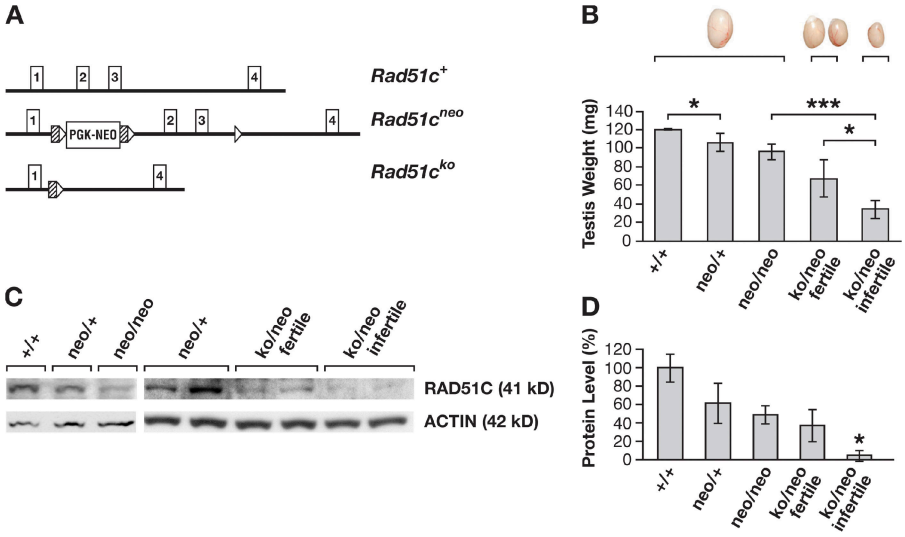

Figure 1. **Effect of the hypomorphic allele on RAD51C protein expression and male infertility.** (A) Schematic representation of *Rad51c* alleles. Only the first four exons are shown (Leasure et al., 2001). In the *Rad51c*^{neo} allele, a *PGK-neo* cassette flanked by *FRT* (hatched boxes) and *loxP* (open triangles) sites is inserted into intron 1, and another *loxP* site is inserted into intron 3. The *Rad51c*^{ko} allele is a product of Cre-mediated recombination at *loxP* sites, resulting in a deletion of exons 2 and 3. (B) Graph showing the correlation between the *Rad51c* genotype, fertility status, and testes size. Error bars indicate SD from the mean of the testes size for respective genotypes. Asterisks represent the statistical significance of the differences between the pairs of genotypes indicated by brackets: *, $P < 0.05$; ***, $P < 0.001$. Examples of testes in relative proportions are shown above the graph. (C) Correlation between the protein level of RAD51C in testes by Western blot analysis and genotype of the mice. (D) Quantitative evaluation of the Western blot shown in C. The histogram represents the amount of RAD51C protein in the testes of mice of various genotypes relative to wild type.

code for a 142–amino acid region, including a linker and the Walker A ATPase domain. The deletion of these exons resulted in a functionally null allele, *Rad51c*^{ko}, which caused an early postimplantation lethality of *Rad51c*$^{ko/ko}$ mouse embryos (unpublished data). In addition to a null allele, we also generated a hypomorphic allele, *Rad51c*^{neo}, by inserting a neomycin (neo) resistance gene under the control of a phosphoglycerate kinase (PGK) promoter into intron 1 (Fig. 1 A). Disruption of normal splicing by the presence of the *PGK-neo* cassette has been reported previously for other genes (Meyers et al., 1998). Aberrant splicing was demonstrated for the *Rad51c*^{neo} allele by RT-PCR analysis using primers to amplify a region between the first and fourth exons (Fig. S1, available at http://www.jcb.org/cgi/content/full/jcb.200608130/DC1). The sequence analysis predicted that the misspliced transcript was likely to encode for a 76–amino acid polypeptide that included 39 amino acids from the first exon of *Rad51c* and an additional 37 amino acids from the 3′ region of the *PGK-neo* cassette. Aberrant splicing resulted in an ∼60% reduction in RAD51C protein levels (Fig. 1, C and D). The combination of a hypomorphic and a null allele (*Rad51c*$^{ko/neo}$) produced mice expressing only 5–30% of the normal level of RAD51C protein (Fig. 1 D).

Infertility in males and females

The residual amount of RAD51C protein in *Rad51c*$^{ko/neo}$ mice is sufficient to allow normal growth and development. However, 36.6% (n = 82) of such males and 11.6% (n= 173) of the females were infertile. In the control group, which included wild type, *Rad51c*$^{ko/+}$, *Rad51c*$^{neo/+}$, and *Rad51c*$^{neo/neo}$ (from here on, these genotypes are referred to as controls for simplicity), only one male and one female out of 105 mating pairs were infertile. To determine the fertility status, 6–8-wk-old *Rad51c*$^{ko/neo}$ mice were mated with wild-type mice for up to 6 wk. Infertile *Rad51c*$^{ko/neo}$ animals were sexually active as indicated by the repeated detection of vaginal plugs, which did not result in pregnancy. In contrast, fertile *Rad51c*$^{ko/neo}$ males and females produced normal sized litters compared with the control group (7.1 ± 2.7 pups [n = 68] and 7.3 ± 2.6 pups [n = 21], respectively).

Meiotic defects in males

Testes of infertile *Rad51c*$^{ko/neo}$ males were significantly reduced in size (P = 0.042) and weighed 18–48 mg at 8–10 wk of age in contrast to 43–90 mg for fertile *Rad51c*$^{ko/neo}$ males. Furthermore, testes of infertile males also had reduced levels of RAD51C protein compared with that of fertile males (Fig. 1, B and C). Unlike testes of the control males, histological examination of testes from 4-wk-old *Rad51c*$^{ko/neo}$ males revealed seminiferous tubules that were deformed and were often almost devoid of germ cells (Fig. 2, A and B). There was a marked increase in the number of apoptotic spermatocytes in the testes of infertile mice as determined by TUNEL assay (Fig. 2, C and D). Testis histology of the 12-wk-old infertile *Rad51c*$^{ko/neo}$ males revealed a few tubules containing some mature spermatozoa, but the majority still showed abnormal structures compared with control testes (Fig. 2, E–H). Seminiferous tubules from control animals were comprised mostly of multiple layers of round spermatids and usually a single layer of spermatocytes undergoing meiotic divisions (Fig. 2 G). In contrast, most tubules from mutant males contained no mature sperm, few, if any, spermatids, and multiple layers of spermatocytes in the zygotene and pachytene stages of meiotic prophase (Fig. 2 H). Although testes morphology and cell composition improved with age, adult males remained functionally infertile for up to 8 mo of age.

To determine the precise nature of spermatogenesis failure in *Rad51c*$^{ko/neo}$ mice, we analyzed surface spreads of spermatocytes using molecular markers specific for different stages of meiosis. SCP3 and SCP1, which are components of the lateral and central elements of the synaptonemal complex, respectively, were used to identify cells at different stages of meiotic prophase based on the degree of chromosome condensation and

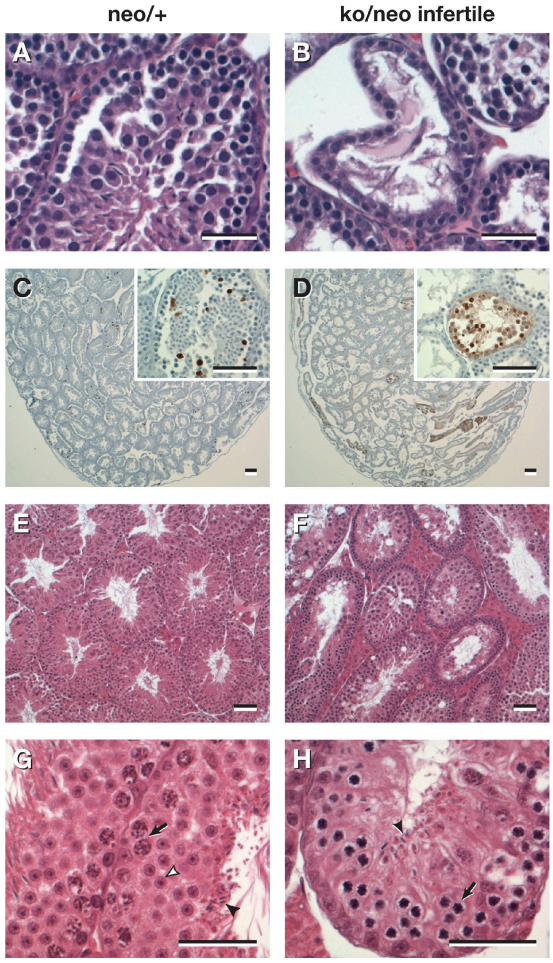

Figure 2. **Histological analysis of the testes of *Rad51c*-deficient mice.** (A and B) Testes from a 4-wk-old *Rad51c*$^{neo/+}$ mouse (A) and its *Rad51c*$^{ko/neo}$ (B) mutant littermate. Note the irregular shape of the seminiferous tubules and the almost complete depletion of meiocytes in the mutant testis. (C and D) TUNEL staining reveals elevated levels of apoptosis in the testis of a 4-wk-old *Rad51c*$^{ko/neo}$ mouse (D) as compared with a *Rad51c*$^{neo/+}$ littermate (C). Insets show higher magnifications of cross sections through TUNEL-positive seminiferous tubules. (E–H) Testes from a 12-wk-old *Rad51c*$^{neo/+}$ male (E and G) and its infertile *Rad51c*$^{ko/neo}$ littermate (F and H). In contrast to the control (G), very few spermatozoa (closed arrowheads) and rare spermatids (open arrowhead) were seen in testes of mutant mice. In addition, multiple layers of primary spermatocytes were also found in mutant mice (H). Arrows in G and H indicate the layers of primary spermatocytes. Interstitial tissues appeared hypertrophied in both infertile (F) and fertile *Rad51c*$^{ko/neo}$ testes. Bars, 20 μm.

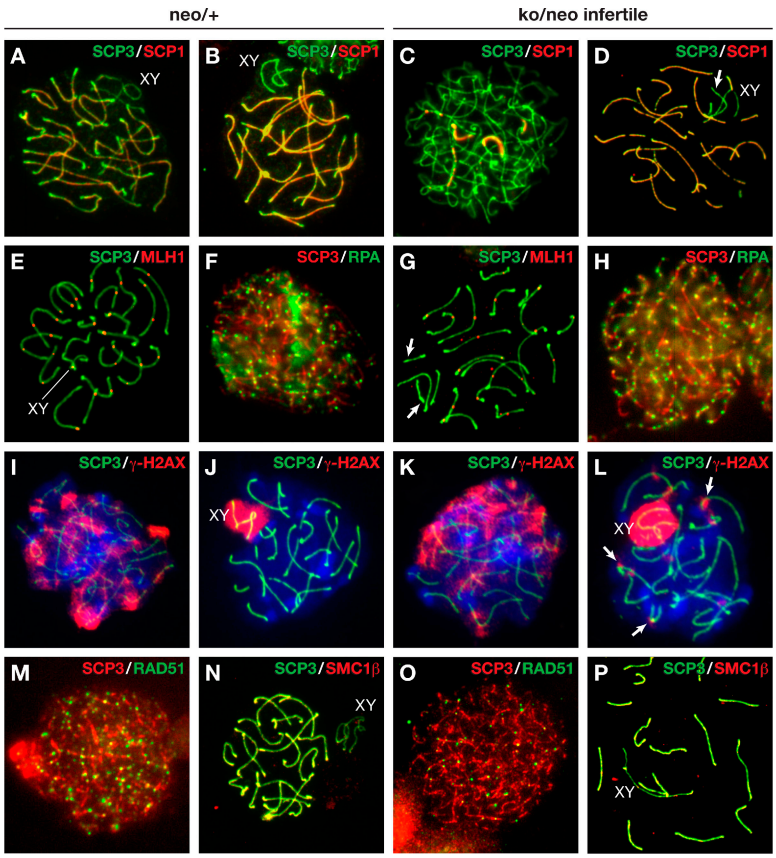

Figure 3. **Meiotic prophase I analysis in infertile *Rad51c*$^{ko/neo}$ males.** The left two columns represent control *Rad51c*$^{neo/+}$ (neo/+) spermatocytes, and the right two columns represent spermatocytes from infertile *Rad51c*$^{ko/neo}$ (ko/neo infertile) littermates. Nuclei were stained with SCP3 antibody (green; except in F, H, M, and O, where SCP3 is in red). XY marks the sex chromosomes. (A–D) Immunostaining for SCP3 and SCP1 shows early prophase I arrest of mutant spermatocytes. Cells at early and midzygotene (C) were predominant in the mutant testes, whereas nuclei at late zygotene (A) and pachytene (B) composed the major population in control testes. Some mutant spermatocytes progressed to pachytene (D) and showed unsynapsed (arrow) chromosomes. (E and G) At pachytene, chiasmata are formed in control spermatocytes (E) as marked by MLH1 staining. Mutant spermatocytes at pachytene often display a few chromosomes lacking MLH1 foci (G). Such chromosomes are highlighted with arrows. (F and H) RPA staining, which marks the initiation of DSB repair, did not differ between control (F) and mutant (H) spermatocytes. (I–L) γ-H2AX staining shows no difference at the zygotene stage between mutant (K) and control spermatocytes (I). At pachytene, γ-H2AX staining is restricted to the sex chromosomes in control spermatocytes (J), but, in *Rad51c* mutants, additional foci (arrows) were present, indicating sites of unrepaired DNA breaks (L). (M and O) RAD51-mediated DSB repair is affected in *Rad51c* mutant spermatocytes. A marked reduction in the number of RAD51 foci was observed at leptotene in mutant spermatocytes (O) compared with the control (M). (N and P) Localization of meiotic cohesins is not affected in mutant spermatocytes as exemplified by normal SMC1β staining at pachytene.

synaptonemal complex formation (Dobson et al., 1994). In control samples, >60% (n = 184) of the spermatocyte population is comprised of cells at late zygotene, when chromosomes are not fully synapsed at their ends (Fig. 3 A), and at pachytene when synapsis is complete (Fig. 3 B). In infertile *Rad51c*$^{ko/neo}$ mutants, we found that some spermatocytes progressed to the pachytene stage (Fig. 3 D), but 63% displayed reduced numbers of MLH1 foci (Fig. 3 G and Fig. S2, B–E; available at http://www.jcb.org/cgi/content/full/jcb.200608130/DC1), which are markers of the crossover sites (Baker et al., 1996). In contrast, only 11% of the control spermatocytes lacked MLH1 foci on one or more chromosomes, whereas most spermatocytes displayed one or two foci on each chromosome (Fig. 3 E and Fig. S2, A and E). Mutant spermatocytes lacking MLH1 are likely to be at the pre-MLH1 early pachytene stage (Fig. S2 D). Overall in mutant *Rad51c*$^{ko/neo}$ males, a shift in spermatocyte distribution toward early stages of prophase I was observed (Table I). The number of late zygotene and pachytene spermatocytes was reduced to 40% (n = 208), whereas cells at leptotene (22% in the mutant vs. 7.6% in the control) and at early to midzygotene (30% in the mutant vs. 21% in the control) became the major fractions (Fig. 3 C). The fact that cells at all stages (leptotene-pachytene) of meiosis could be found in these preparations suggests that the phenotype observed in infertile *Rad51c*$^{ko/neo}$ males reflects an impairment of spermatogenesis during meiosis I rather than an absolute developmental arrest.

Formation and repair of DNA double strand breaks (DSBs) by homologous recombination ensures a correct pairing and subsequent segregation of homologous chromosomes during the first meiotic division. A successful generation of DSBs and initiation of their repair is indicated by the presence of phosphorylated histone H2AX (γ-H2AX; Fig. 3, I and K) and RPA (Fig. 3, F and H) protein staining in mutant and control spermatocytes at leptotene and zygotene (Plug et al., 1997; Mahadevaiah et al., 2001). At pachytene, normally only the sex chromosomes stain positively for γ-H2AX (Fig. 3 J; Mahadevaiah et al., 2001). However, in mutants, more than half of all spermatocytes displayed multiple γ-H2AX foci at pachytene, indicating the persistence of DSBs at this stage (Fig. 3 L). We found no marked difference in the number of RPA foci in mutant and control spermatocytes at various stages of prophase I (Fig. 3, F and H; and Fig. S3, available at http://www.jcb.org/cgi/content/full/jcb.200608130/DC1). As RAD51C has been implicated in RAD51 foci formation in mitotic cells, we tested whether RAD51 foci formation was defective in spermatocytes of infertile males. RAD51 plays an important role in the initial steps of homologous recombination by mediating homologous pairing and strand exchange and is normally observed in multiple foci first appearing at leptotene and sharply decreasing at pachytene (Fig. S4, A–C; Ashley et al., 1995). We found that the number of RAD51 foci was reduced about threefold at leptotene and zygotene stages in spermatocytes of *Rad51c*$^{ko/neo}$ 3-mo-old mice (46–57 foci per cell in the mutant compared with 140–169 foci in the *Rad51c*$^{neo/+}$ littermate control; Fig. 3, M and O; and Fig. S4, D–G), indicating an early defect in the homologous recombination process.

Table I. **Stage distribution of spermatocytes from *Rad51c*$^{ko/neo}$ males in prophase I**

Genotype	Leptotene	Early zygotene	Late zygotene/pachytene	Diplotene/diakinesis
	%	%	%	%
ko/+	8	21	60 (mostly P)	11
ko/neo	22	30	40 (mostly LZ)	8

Mutant spermatocytes undergo early arrest during prophase I. 184 and 208 spermatocytes stained for SCP3/SCP1 were counted in control and mutant samples, respectively. LZ, late zygotene; P, pachytene.

γ-H2AX staining marks not only unrepaired DNA but also unsynapsed regions along homologous chromosomes. Although some mutant spermatocytes showed only a few γ-H2AX foci on autosomal chromosomes, we found others that had entire chromosomes staining positively for γ-H2AX at pachytene (Fig. 4 A, arrowheads). Such chromosomes also appeared thinner than others when stained for SCP3 (Fig. 4 B, arrowheads) and lacked SCP1 staining (Fig. 3 D, arrow), suggesting that these were completely unpaired autosomal univalents. Abnormal synapsis between homologous chromosomes was further confirmed by karyotyping spermatocytes at metaphase I. We examined metaphase I spermatocytes from 3-wk-old *Rad51c*$^{ko/neo}$ males, which were potentially infertile as identified by testes weight, and a *Rad51c*$^{neo/+}$ littermate control. We found that although a few metaphase I spermatocytes (16%; $n = 114$) from mutant males appeared normal, similar to the control spermatocytes (Fig. 4, C and D), the majority (84%) were morphologically abnormal, possibly undergoing apoptotic fragmentation of the chromatin (Fig. 4, E and F). Unpaired autosomal univalents were visible in each of these spreads (Fig. 4, E and F; arrowheads). Such univalents are known to induce apoptosis at metaphase I (Eaker et al., 2001). Although metaphase I and II spermatocytes were almost equally represented in control animals (57% and 43%, respectively; $n = 90$), metaphase II spermatocytes were rarely found in mutant males (9%; $n = 125$). This suggests that mutant spermatocytes rarely progress beyond metaphase I, as they undergo apoptosis at this stage.

Meiotic defects in females

Ovaries from infertile females were similar in size compared with fertile littermates, and histological examination showed the presence of morphologically normal follicles at all stages of development (Fig. 5, A–F). However, ovaries from 6- and 12-wk-old animals revealed the absence of corpora lutea in infertile *Rac51c*$^{ko/neo}$ females, suggesting that failure to ovulate may be the cause of infertility (Fig. 5, D and E). This ovulation block could be overcome by hormonal (intraperitoneal injection of 5 IU [0.1 cc] of pregnant mare serum [PMS] followed by a second injection of 5 IU [0.1 cc] of human chorionic gonadotropin [hCG] 48 h later) treatment (see ovary histology after superovulation; Fig. 5 F), after which infertile *Rad51c*$^{ko/neo}$ females could become pregnant when mated with wild-type males. When embryos from the uterine horns of these mice were dissected at embryonic day 8.5, we found that the number of embryos obtained from infertile *Rad51c*$^{neo/ko}$ females was greatly reduced (5 ± 0; $n = 2$) compared with the number of embryos from heterozygous *Rad51c*$^{neo/+}$ superovulated littermates (15.5 ± 4.94; $n = 2$; $P = 0.05$). In addition, 7/10 embryos (70%) from the mutant females displayed a wide range of developmental abnormalities compared with only two abnormal embryos out of 31 (6.5%) from superovulated control mice (Fig. 5 H). All of the embryos from the control females appeared to develop normally (Fig. 5 G). We hypothesized that the developmental defects observed in these embryos resulted from gross chromosomal defects in the oocytes caused by abnormal meiosis (Yuan et al., 2002).

To determine the cause of such abnormalities in oocytes, we examined the meiotic progression of germinal vesicle (GV)–intact oocytes by in vitro maturation. Chromosomes of the control *Rad51c*$^{neo/+}$ oocytes were aligned at the metaphase plate after 8 h of maturation (Fig. 5 I). Mutant oocytes progressed to metaphase I, and some aligned normally along the metaphase plate (Fig. 5 K). However, 60–75% ($n = 50$) of them displayed

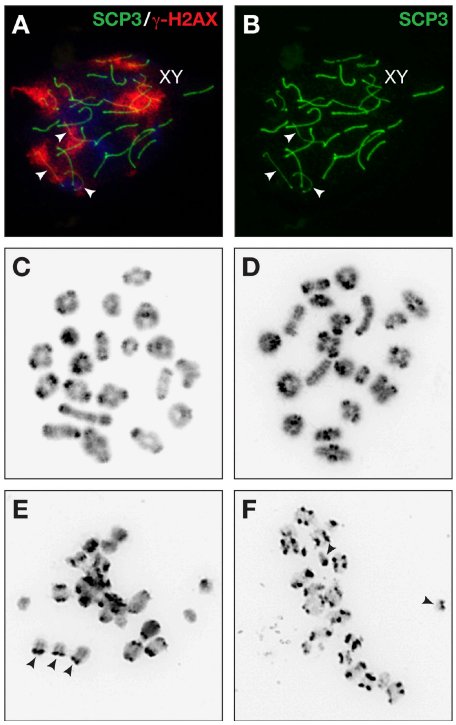

Figure 4. **Univalents are frequently found in mutant spermatocytes that progress to metaphase I.** (A and B) SCP3 (green) and γ-H2AX staining (red) indicate the presence of a few completely unsynapsed chromosomes in infertile *Rad51c*$^{ko/neo}$ spermatocytes as early as pachytene. Arrowheads mark unsynapsed chromosomes or univalents. (C–F) Metaphase I spreads of spermatocytes from control *Rad51c*$^{neo/+}$ (C) and mutant males (D–F). A few mutant spermatocytes display proper pairing of homologous chromosomes (D), but the majority shows the presence of univalents (arrowheads in E and F). The abnormal appearance of chromosomes in the spreads containing univalents may indicate their apoptotic DNA degradation.

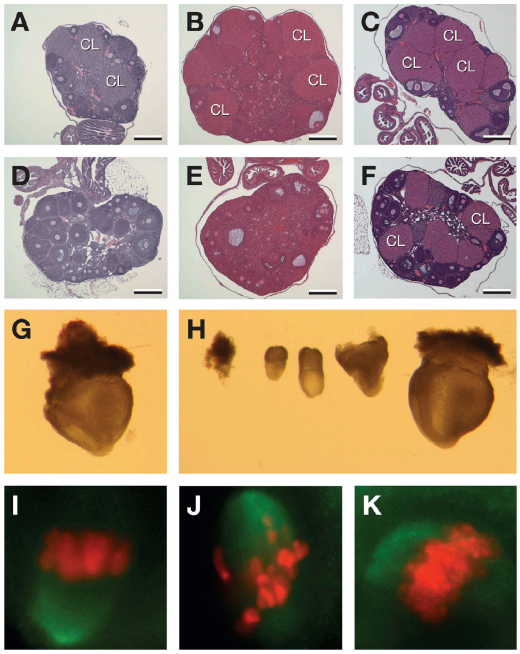

Figure 5. **Fertility defect and meiotic progression in *Rad51c* mutant females.** (A–F) Histology of ovaries showing an ovulation defect in infertile *Rad51c*$^{ko/neo}$ females. In contrast to control females (A and B), no corpora lutea (CL) were seen in ovaries from infertile *Rad51c*$^{ko/neo}$ females at 6 (D) or 12 wk (E) of age. However, successful ovulation was achieved after hormone treatment from control (C) and mutant (F) ovaries. Note that there are still fewer corpora lutea in mutant ovaries after the superovulation procedure (F). Bars, 200 μm. (G and H) Infertile *Rad51c*$^{ko/neo}$ females produce developmentally abnormal embryos after superovulation. Only one out of five embryonic day 8.5 embryos produced by an infertile *Rad51c*$^{ko/neo}$ female (H) appeared comparable with a control embryo (G). (I–K) Large portion of oocytes from mutant females revealed improperly aligned chromosomes at metaphase I (J) after 8 h of in vitro maturation compared with control heterozygous littermates (I). Some oocytes from mutant females do show a normal alignment of chromosomes at the metaphase plate (K). The chromosomes were stained by DAPI. For better visualization, the blue DAPI staining has been converted to red. The green signal represents the spindle microtubules.

poorly structured metaphase plates (Fig. 5 J) in contrast to only 30% (n = 33) of abnormal oocytes from control *Rad51c*$^{neo/+}$ littermates. The reason for the relatively high number of abnormal oocytes observed in control samples is unclear. One possibility is that this might be an effect of haploinsufficiency, as these animals were heterozygous for the hypomorphic allele.

We examined the karyotypes of metaphase I oocytes, which revealed no apparent defects in pairing and cohesion in infertile *Rad51c*$^{ko/neo}$ females (n = 8) compared with the oocytes from *Rad51c*$^{neo/+}$ females (n = 6; Fig. 6, A and B). Evaluation of the centromeric cohesion between sister chromatids was facilitated by using a centromere-specific probe (Fig. S5, A and B; available at http://www.jcb.org/cgi/content/full/jcb.200608130/DC1). We then karyotyped the oocytes that were allowed to progress to metaphase II in vivo after hormonal treatment. At metaphase II, oocytes from fertile females show the presence of 20 pairs of chromatids, each consisting of two sister chromatids that are attached together at their centromeres (Fig. 6 C). In oocytes from infertile *Rad51c*$^{ko/neo}$ mice, we found a variety of chromosomal abnormalities. A majority of the mutant oocytes (85%; n = 34) showed precocious separation of sister chromatids (PSSC), indicating a problem with chromatid cohesion (Fig. 6 D). The degree of the cohesion defect varied from cases in which all chromosomes were affected (approximately half of all cases) to those in which only a few chromosomes were affected (for more examples, see Fig. S5, D–G). Only one oocyte from the control littermate was found to have a PSSC phenotype (5%; n = 20). Mutant oocytes with a PSSC phenotype often had a few acentric chromatids (40%; n = 10; Fig. 6 D, open arrowhead; and Fig. S5 F, arrowheads). On the other hand, a few other chromatids in the same spreads had two centromeres (Fig. 6 D, double arrows; and Fig. S5, E–G; double arrows). No such phenotype was observed in control oocytes. In addition, 20% of mutant oocytes (n = 10) in which chromosomes could be counted revealed >20 chromosomes or chromatid pairs, whereas others had 20 or fewer pairs of centromeres, indicating the abnormal segregation of homologous chromosomes during anaphase I of meiosis (Fig. S5 G).

The chromosomal defects observed in oocytes after metaphase I suggest a late role for RAD51C in recombinational repair. We did not find any evidence to support a direct role of RAD51C in sister chromatid cohesion (see Discussion; unpublished data). However, based on a biochemical study (Liu et al., 2004), the late function of RAD51C is likely to be associated with the resolution of HJs. To test whether HJ resolvase activity is indeed affected in *Rad51c*-deficient mouse cells, we examined protein extracts from mouse embryonic fibroblasts (MEFs) in an in vitro HJ resolution assay. Two *Rad51c*$^{ko/ko}$ MEF lines were established on a *p53*-null background, which partially rescued the early embryonic lethality of *Rad51c*-null embryos (unpublished data). We used MEFs derived from *p53*-null and wild-type embryos as controls. HJ resolution activity of protein extracts from the two *Rad51c* mutant MEFs was at the background levels between 1.9 and 3.8% and did not correlate with the increasing amounts of protein extract (Fig. 6, E and F). The HJ resolution activity of the *p53*-null control cells increased from 5.4 to 11.3% as the amount of protein extract increased from 0.9 to 3.5 μg. This was slightly higher than the activity of the wild-type primary MEFs (between 1.0 and 7.5%; Fig. 6, E and F). These activity differences correlated with the amount of RAD51C protein detected in these extracts by Western blotting (Fig. 6 G). Thus, these data further support a RAD51C role in the resolution of HJs.

Spermatocytes at metaphase II

To test whether the premature separation of chromatids occurred even in males, we examined the spermatocytes that progressed to metaphase II (n = 39 in control and n = 11 in mutant samples). In control spermatocyte samples, we found 20 pairs of chromatids attached at the centromeres as observed in oocytes (Fig. 7 A and Fig. 6 C, respectively). Although the chromosomes in some mutant spermatocytes appeared to be normal (Fig. 7 B), others revealed fragmented chromosomes with broken centromeres or had aberrant chromosome numbers (Fig. 7, C and D). However, none of the mutant spermatocytes displayed the sister chromatid cohesion defect. Thus, the PSSC defect is a sexually dimorphic feature restricted only to females. It is unclear

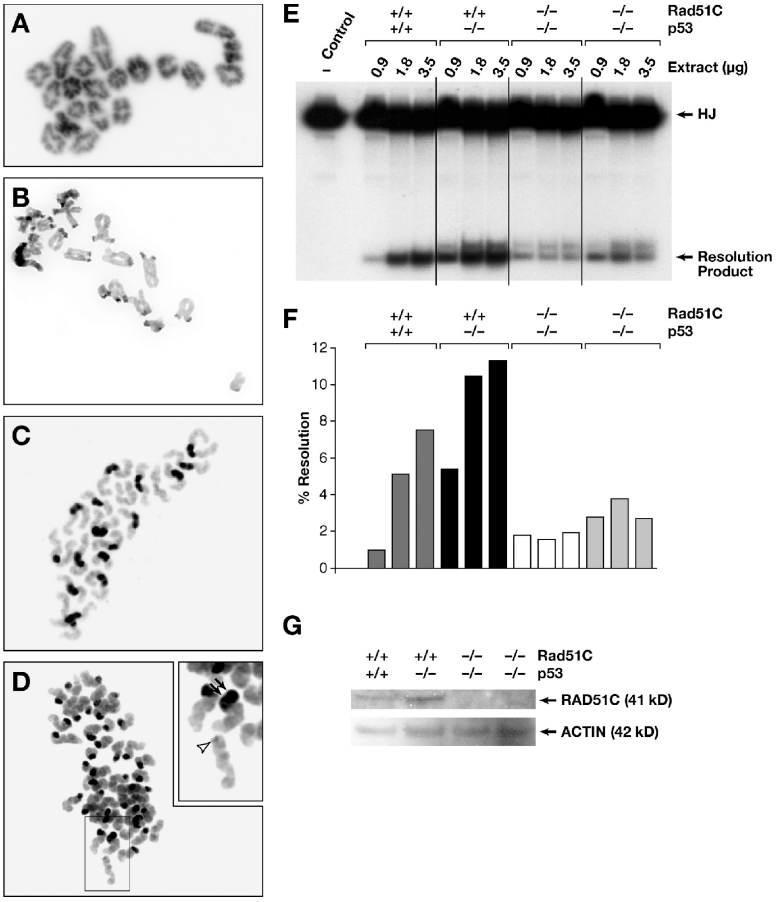

Figure 6. **A late role for RAD51C in meiotic recombination is revealed at metaphase II.** (A and B) Metaphase I chromosomes in control (A) and mutant (B) oocytes appear karyotypically normal and show normal pairing and chiasmata formation. (C and D) At metaphase II, unlike oocytes from control littermates (C), most oocytes from infertile *Rad51c*$^{ko/neo}$ females (D) show abnormal sister chromatid cohesion and broken chromosomes. The inset in D is a higher magnification image of the group of chromosomes showing an acentric chromatid (arrowhead) and a chromatid with two centromeres (double arrows). (E) Protein extracts from *Rad51c*-null MEFs reveal reduced HJ resolvase activity compared with control MEFs. HJ indicates the [^{32}P]end-labeled synthetic HJ DNA substrate. (F) Quantitative representation of the results shown in E. (G) Western blot examination of the RAD51C protein level in extracts from MEFs used for HJ resolution assay.

whether this phenotype in males is caused by a defect in DSB repair or is caused by the defect in HJ resolution. We present a model to explain how a defect in HJ resolution may result in PSSC in oocytes (see Discussion and Fig. 8).

Discussion

Early role of RAD51C in mouse meiosis

To date, the only well established function of RAD51C is its role in the process of homologous recombination by facilitating RAD51 foci formation after DNA damage. The precise role of RAD51C in the recruitment of RAD51 and how it differs from other RAD51 paralogues is still unclear. More importantly, recent studies of *AtRad51c*- and *AtXrcc3*-deficient *Arabidopsis* plants and fruit flies deficient in a RAD51C-like gene, *spn-D*, point to their unique requirement in meiosis unlike other RAD51 paralogues (Abdu et al., 2003; Bleuyard et al., 2005). Characterization of the *AtRad51c* mutant plants showed that this defect is associated with the repair of Spo11-induced DSBs, leading to abnormal synapsis and severe chromosomal fragmentation at the pachytene stage of prophase I (Abdu et al., 2003; Li et al., 2005).

In this study, we describe a meiotic defect in *Rad51c* mutant male mice that is associated with abnormal synapsis between homologous chromosomes at pachytene. At this stage, abnormal synapsis is indicated by the presence of γ-H2AX foci on some of the autosomal chromosomes. Occasionally, entire chromosomes appeared positive for γ-H2AX, indicating completely unsynapsed chromosomes (Fig. 4, A and B). Unlike *Arabidopsis*, mouse spermatocytes with unsynapsed chromosomes undergo apoptosis either at pachytene or metaphase I

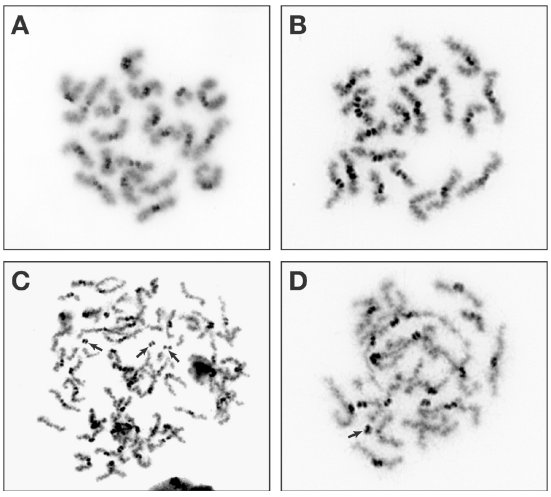

Figure 7. **Rad51c mutant spermatocytes reveal chromosome fragmentation but no PSSC defect at metaphase II.** (A) Spermatocyte from a control male at metaphase II showing 20 pairs of sister chromatids attached at their centromeres. (B–D) Metaphase II spreads from a *Rad51c*$^{ko/neo}$ infertile male. Although some spermatocytes appear to be normal (B), others reveal broken centromeres (indicated with arrows) and aberrant chromosome numbers (C). Unlike oocytes, the PSSC defect was not observed in mutant spermatocytes.

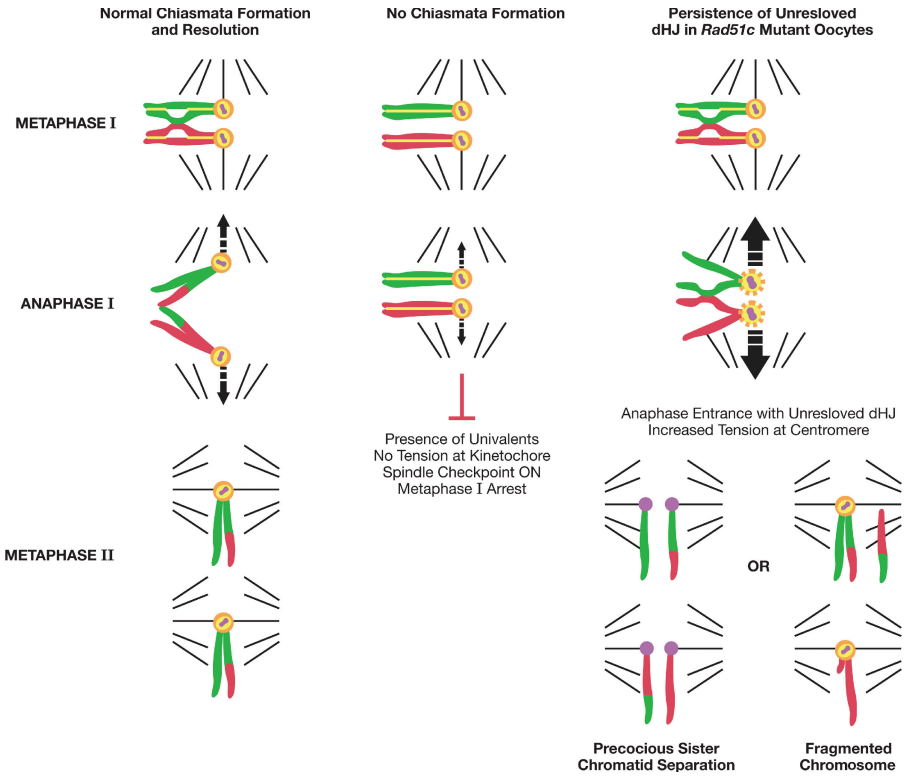

Figure 8. **Model demonstrating a proposed connection between the HJ resolution defect and abnormalities found in *Rad51c* mutant oocytes at metaphase II.** See Discussion for details. Homologous chromosomes are shown in red and green. REC8 is shown in yellow, Sgo1 is depicted in orange, and centromeres are shown in purple.

(Mahadevaiah et al., 2000; Eaker et al., 2001). Consistent with this, we observed a massive increase in abnormal metaphase I spermatocyte spreads.

Chromosome synapsis is dependent on RAD51-mediated recombination machinery, which helps bring homologous chromosomes together to repair DNA breaks introduced at leptotene using homologous regions as a template. We found that in *Rad51c*$^{ko/neo}$ spermatocytes, the number of RAD51 foci was reduced about threefold as early as at leptotene. This is consistent with observations of attenuated RAD51 foci formation in RAD51C-deficient cell lines and with a recent finding that RAD51C may interact with RAD51 directly or as a complex with XRCC3 (Eaker et al., 2001; Rodrigue et al., 2006). A similar role for Rad55/Rad57, the budding yeast paralogues of RAD51, has been described previously (Gasior et al., 2001). The lack of RAD51 foci revealed in spermatocytes of *Brca2*-deficient mice results in developmental arrest at late zygotene (Sharan et al., 2004). However, *Rad51c*$^{ko/neo}$ spermatocytes do not completely arrest at this stage but clearly accumulate at leptotene and at early to midzygotene. This suggests that the RAD51C defect in these mice causes impairment of the RAD51 function; however, because of the hypomorphic nature of the mutation, some spermatocytes escape an early arrest at zygotene, progress further with unrepaired DSBs, and exhibit partially or completely unsynapsed chromosomes so that most of them are eventually blocked at metaphase I.

Late role of RAD51C in mouse meiosis

Like the males, a subset of the *Rad51c*$^{ko/neo}$ females failed to produce any litters. Female infertility was associated with an ovulation failure, as no corpora lutea were found in ovaries of such mice. In ovaries of adult mice, oocytes are normally arrested in meiotic prophase I (Borum, 1961). As ovaries of the infertile *Rad51c*$^{ko/neo}$ mice were of the same size as the wild-type animals and contained follicles at all stages of maturation, we conclude that *Rad51c*-deficient oocytes are able to progress to pachytene normally without an early arrest like in males.

However, oocytes from infertile *Rad51c*$^{ko/neo}$ mice do suffer a maturation defect preventing ovulation, which could be overcome only by external hormonal stimulation. Although the number of GV-intact oocytes isolated from ovaries of such females was not considerably reduced compared with littermate controls, they often appeared more fragile to handle during the in vitro maturation experiments (unpublished data). Mutant oocytes display other early meiotic defects like an increased incidence of dysregulated chromosome alignment at the metaphase plate during metaphase I. Such defects may result from the impaired DSB repair as observed in mutant spermatocytes, but, unlike spermatocytes, oocytes could progress to metaphase I even with unrepaired DSBs as a result of sexually dimorphic checkpoint mechanisms (Eaker et al., 2001; Hunt and Hassold, 2002). Sexually dimorphic phenotypes in mice have been reported for several other meiotic mutations. Mutations in genes like *Scp3*, *Mei1*, and *Brca2* result in male meiosis arrested during a zygotene to pachytene transition, whereas mutant oocytes can progress through pachytene all the way to metaphase I (Libby et al., 2002; Yuan et al., 2002; Sharan et al., 2004). Similarly, sexual dimorphism in *Rad51c*-deficient mice is reflected by the fact that 37% of *Rad51c*$^{ko/neo}$ males were infertile, whereas only 12% of females were infertile.

Despite a slightly dysregulated chromosome alignment at the metaphase plate, mutant oocytes were karyotypically

normal and did not display unsynapsed chromosomes, which is characteristic of metaphase I oocytes with early meiotic dysfunctions (such as MLH1 and Mei1-deficient mice; Woods et al., 1999; Libby et al., 2002). Thus, abnormal embryos produced by infertile females after superovulation must be caused by defects occurring after the metaphase I stage. Indeed, major chromosomal abnormalities were found in mutant oocytes later at metaphase II such as PSSC, aneuploidy, and broken chromosomes.

Role in sister chromatid cohesion versus HJ resolution

PSSC is the most prominent defect at metaphase II, affecting almost all oocytes of the *Rad51c* mutant infertile females. The PSSC phenotype has been previously demonstrated for several genes regulating meiotic cohesion such as *SMC1β* in mice and Sgo1, Bub1, and PP2A in yeast (Bernard et al., 2001; Kitajima et al., 2004; Revenkova et al., 2004; Riedel et al., 2006). Sister chromatid cohesion is mediated by the multiprotein complex cohesin, comprising REC8, STAG3, SMC1β, and SMC3 proteins (Prieto et al., 2004). During prophase I of meiosis, cohesin is required for synaptonemal complex formation and recombination to occur between homologous chromosomes rather than between sister chromatids (Schwacha and Kleckner, 1997). Although cohesin is cleaved and released from chromosome arms by separase at metaphase I, Shugoshin protects it at centromeres until anaphase II (Fig. 8; Wang and Dai, 2005). This ensures a correct segregation of homologues at anaphase I and sister chromatids at anaphase II into separate daughter cells. Mice deficient for meiotic cohesins are infertile and display a wide range of defects, from the failure of interhomologue synapsis and recombination for $Rec8^{-/-}$ mice (Xu et al., 2005) to the occasional breakup of bivalents at metaphase I and premature sister chromatid separation that is detectable at metaphase I and is fully exposed at metaphase II for $SMC1\beta^{-/-}$ mice (Revenkova et al., 2004). This sister chromatid cohesion defect at metaphase II seen in infertile $Rad51c^{ko/neo}$ females is remarkably similar to defects found in *SMC1β* knockout mice (Revenkova et al., 2004). Interestingly, a hamster cell line lacking functional RAD51C has also been reported to have defects in sister chromatid cohesion (Godthelp et al., 2002). Altogether, these findings suggested a possible role for RAD51C in sister chromatid cohesion.

We tested whether RAD51C protein can directly interact with proteins involved in sister chromatid cohesion like RAD21, REC8, SMC1β, and Shugoshin (Sgo1) by coimmunoprecipitation but found no evidence to support this hypothesis (unpublished data). This does not eliminate the possibility that RAD51C affects cohesins indirectly via other binding partners or signaling pathways. However, other evidence suggests that RAD51C may not be directly involved in sister chromatid cohesion. First, immunostaining of spermatocyte spreads for SMC1β, RAD21, and REC8 did not reveal any obvious abnormalities during prophase I in male meiosis (Fig. 3, N and P; and not depicted). Second, neither PSSC nor univalents were observed in *Rad51c* mutant oocytes at metaphase I unlike $SMC1\beta^{-/-}$ mice (Revenkova et al., 2004). Third, cohesin failure alone does not explain the presence of acentric chromatids and chromatids with two centromeres seen in the *Rad51c*-deficient oocytes. Fourth, the few mutant spermatocytes that reach metaphase II do not show any defect in sister chromatid cohesion (Fig. 7). Finally, no sister chromatid cohesion defects were found in *Rad51c*-null MEFs generated from $Rad51c^{-/-}$ embryos (unpublished data). On the other hand, in addition to biochemical activity, a role for RAD51C in HJ resolution is supported by its colocalization with MLH1 to the site of an obligate crossover at the pseudoautosomal region of the sex chromosomes and by the observation that the number of RAD51C foci is substantially reduced in spermatocyte spreads of $Mlh1^{-/-}$ mice (Liu et al., 2007). Also, we have shown that protein extracts from *Rad51c*-null MEFs lack HJ resolution activity, which further supports this finding (Fig. 6, E and F).

How does the HJ resolution defect result in PSSC?

If RAD51C indeed plays a role in the resolution of HJ, why do RAD51C mutant oocytes exhibit a sister chromatid cohesion defect? A precise phenotype of an HJ resolvase deficiency in the mouse is difficult to predict because so far no other mouse protein has been implicated in this process. Mus81-Eme1 was identified as an HJ resolvase in fission yeast (Boddy et al., 2001). Yeast cells deficient for any of these genes are sterile as a result of a defect in chromosome segregation. However, in higher eukaryotes, HJ resolution is likely to be performed by other molecules because Mus81-deficient mice are fertile and do not show any meiotic defect (Dendouga et al., 2005). We propose that the PSSC phenotype reflects the response of unresolved chromosomes to the increased tension exerted by the spindle at the kinetochores when the chromosomes are pulled to the opposite poles. This model is supported by the behavior of dicentric chromatids in mouse oocytes, which revealed a range of meiotic defects that were surprisingly similar to those of *Rad51c*-deficient oocytes, including PSSC as well as broken or acentric chromosomes and aneuploidy at metaphase II (Koehler et al., 2002). Such dicentric chromosomes were generated in strains of mice that were heterozygous for an inversion in a large region of chromosomes X or 19. Meiotic recombination in the inverted region led to the generation of dicentric chromatids. When pulled in opposite directions during anaphase I, such chromatids resulted in PSSC in 90–97% of cases and rarely in broken chromosomes (3–10%). Interestingly, the meiotic behavior of such chromosomes in female mice was different from that in male mice, flies, and maize, which were more prone to breakage or selective loss (Koehler et al., 2002). Consistent with this observation, metaphase II spermatocytes from $Rad51c^{ko/neo}$ mutant mice do not show any sister chromatid cohesion defect but do show chromosomes with broken centromeres (Fig. 7, C and D).

We speculate that a similar situation would be created if homologous chromosomes failed to dissolve chiasmata. Chiasmata are the cytological manifestation of crossovers, which are believed to arise from double HJs (Szostak et al., 1983). Therefore, we conclude that the late meiotic defects found in oocytes of infertile $Rad51c^{ko/neo}$ mice can be associated with the HJ resolution failure and propose a model to explain its mechanism (Fig. 8).

In normal meiocytes, HJs are established between homologous chromosomes by the pachytene stage of prophase I using the homologous recombination machinery. At metaphase I, bivalents align in the middle of the spindle so that homologous chromosomes can be pulled in opposite directions by microtubules attached to kinetochores of sister chromatids that are oriented toward the same pole. Correct chromosomal alignment triggers anaphase-promoting complex activation, and cohesion is released along the chromosome arms, whereas Sgo1 protects it at the centromere to ensure that sister chromatids stay together during the reductional division. In fission yeast, a spindle checkpoint regulator, Bub1, is essential for the recruitment of Sgo1 to centromeres and, together with Sgo2, promotes sister kinetochore coorientation during metaphase I (Vaur et al., 2005). After chiasmata are dissolved, homologous chromosomes can segregate in separate cells. When chiasmata are not formed, homologous chromosomes cannot align properly at the metaphase plate. This activates a spindle checkpoint leading to metaphase I arrest (Fig. 8).

We propose that in *Rad51c*-deficient oocytes, meiosis proceeds normally until anaphase I. However, there is an accumulation of recombination intermediates such as double HJs that hold the homologous chromosomes together even though the chiasmata fail to fully mature. At the onset of anaphase, there is an increase in tension at the centromere as a result of the persistence of unresolved double HJs. The increased tension may disrupt sister chromatid cohesion at the centromere, as has been demonstrated for dicentric chromosomes and the unpaired X chromosome of XO mice (Hodges et al., 2001; Koehler et al., 2002). The exact mechanism of this process is unclear. However, centromeric sister chromatid cohesion is sensitive to chemicals interfering with the metaphase I to anaphase I transition (Yin et al., 1998; Mailhes et al., 1999). In addition, Sgo1 has been shown to be a sensor of kinetochore tension in mitotic cells (Indjeian et al., 2005). Although it remains to be shown in meiosis, it is likely that Shugoshin degradation/disruption caused by increased tension plays a critical role in the PSSC phenotype that is so prominent in *Rad51c*-deficient oocytes.

In addition to the disruption of centromeric cohesion, chromosome breakage is another consequence of increased tension. Indeed, half of all *Rad51c*-deficient oocytes displayed broken chromosomes (Fig. 6 and Fig. S5, E–G). We predicted that in such cases, the centromeric cohesion would remain unaffected. As shown in Fig. 6 D (inset), in several oocytes, we did observe single chromatids with an extra centromere that is likely to have originated from a sister chromatid. It is also possible that both homologous chromosomes may segregate into one daughter cell, which would lead to aneuploidy detectable at metaphase II. We did see aneuploidy in 2/10 oocytes in which individual chromosomes could be counted (Fig. S5 G).

Based on the meiotic defects observed in infertile $Rad51c^{ko/neo}$ females, we speculate that RAD51c functions in late stages of meiotic recombination, possibly participating in the resolution of HJs. We cannot rule out the possibility that RAD51C may play a role in sister chromatid cohesion, which may explain the PSSC defect in oocytes. Similarly, it is possible that the primary defect may be the same (i.e., a defect in RAD51-mediated DSB repair) in males and females, but the phenotypes are different because of sexually dimorphic checkpoints. However, based on the evidence presented here, we have proposed a model connecting the impairment of HJ resolution function in $Rad51c^{ko/neo}$ infertile females to the observed phenotype in oocytes.

Materials and methods

Generation of *Rad51c* mutant embryonic stem cells and mice

The $Rad51c^{neo}$ allele was generated in embryonic stem cells in which a *neo* resistance gene flanked by two *loxP* sites was inserted into intron 1 and a single *loxP* was inserted into intron 3. Heterozygous offspring in the C57BL/6J × 129/Sv mixed genetic background were crossed with β-actin–*cre* transgenic mice (Lewandoski et al., 1997) to obtain the $Rad51c^{ko}$ allele. Mutant $Rad51c^{ko/neo}$ mice were generated by crossing $Rad51c^{ko/+}$ or fertile $Rad51c^{ko/neo}$ mice to $Rad51c^{neo/neo}$ mice.

Fertility testing

To determine the fertility status of $Rad51c^{ko/neo}$ mice, 6-wk-old males and females were mated with fertile animals for 4–10 wk. To monitor the mating behavior, mice were checked for vaginal plugs daily in a course of at least 6 wk. Mice that plugged several times but failed to produce any offspring were identified as infertile. Infertile $Rad51c^{ko/neo}$ mice are referred to as mutant mice in the text for simplicity.

Western blotting

Protein lysates from control and mutant testes were prepared in cold radioimmunoprecipitation assay buffer. Samples containing 80 μg of protein were separated in NuPAGE 4–12% Bis-Tris polyacrylamide gels (Invitrogen) and transferred onto a nylon membrane. The membrane was probed with mouse or rabbit α-RAD51C antibody (Novus Biologicals or Chemicon International, respectively) at a 1:500 dilution or were probed with α-panactin antibody (NeoMarkers) diluted 1:400 according to standard procedures. Secondary α-mouse IgG-HRP antibody (1:2,000; Santa Cruz Biotechnology, Inc.) and an ECL chemiluminescence system (GE Healthcare) were used for signal visualization.

Histology

Testes and ovaries were fixed in Bouin's solution. Samples were dehydrated through an ethanol series, embedded in paraffin, serially sectioned, and stained with hematoxylin and eosin. Slides were examined using brightfield microscopy. For TUNEL staining, testes were fixed in 10% neutral buffered formalin and were stained using the ApopTag kit (Chemicon International) according to the manufacturer's instructions.

Spermatocyte spread preparation and immunofluorescence

Surface spreads of spermatocytes from the testes of mutant and control animals were prepared and stained as described previously (Romanienko and Camerini-Otero, 2000). Another method was used to prepare spermatocytes for the RAD51 and RPA staining and was described previously (Counce and Meyer, 1973). The difference between the two protocols is that no enzymatic treatment is involved in the second method, and cells are separated by pipetting and spread in a hypotonic solution directly on a slide. The following primary antibodies were used for immunofluorescence: rabbit anti–γ-H2AX (1:1,000; obtained from W. Bonner, National Cancer Institute, Bethesda, MD), mouse anti-MLH1 (1:10; BD Biosciences), rabbit polyclonal α-SCP3 (1:500), α-SCP1 (1:1,000), α-RPA (1:100; all provided by P. Moens, York University, Toronto, Canada), mouse monoclonal α-SMC1β (1:10; provided by E. Revenkova, Mount Sinai School of Medicine, New York, NY), and rabbit α-Rad51 (1:500; obtained from S. West, Cancer Research UK, South Mimms, UK). Secondary antibodies used were goat anti–rabbit AlexaFluor488, goat anti–rabbit AlexaFluor568, goat anti–mouse AlexaFluor488, and goat anti–mouse AlexaFluor568 (Invitrogen). Secondary antibodies were used at a 1:250 dilution.

Image acquisition

Images were acquired with a microscope (Axioplan 2; Carl Zeiss MicroImaging, Inc.) using an oil plan Neofluar 100× 1.3 NA objective (Carl Zeiss MicroImaging, Inc.). Images were taken with a CCD camera (Quantix; Photometrix) and processed using SmartCapture software (Desksoft). Images were further processed with Photoshop software (Adobe) to adjust for size and contrast.

Superovulation and collection of oocytes and embryos

Females were superovulated, and oocytes and embryos were collected as described previously (Hogan et al., 1994). In brief, 0.1 ml PMS (5 IU; Sigma-Aldrich) was injected intraperitoneally into female mice. GV-intact stage oocytes were collected 44–48 h later in flushing and holding medium with 3 mg/ml BSA (Specialty Media) by puncturing ovaries with a 27-gauge needle. Oocytes were incubated briefly in 0.1 mg/ml hyaluronidase type IV-S (Sigma-Aldrich), and cumulus cells were removed by pipetting before transfer into Chatot, Ziomek, and Bavister media containing L-glutamate and 3 mg/ml BSA (Specialty Media) for 8 h at 37°C and 5% CO_2 to obtain metaphase I stage oocytes for immunocytochemistry and karyotyping. Alternatively, 48 h after PMS treatment, 6-wk-old female mice were given an intraperitoneal injection of 0.1 ml hCG (5 IU; Sigma-Aldrich), and, 14 h later, metaphase II–stage oocytes were collected from ampullae. To obtain embryos, 6-wk-old female mice given both PMS and hCG injections were placed with stud males.

Immunocytochemistry of oocytes

Metaphase I and II stage oocytes were washed in Dulbecco's PBS without $CaCl_2$ or $MgCl_2$ (Invitrogen) and were fixed for 10 min in cold methanol. Oocytes were incubated in blocking buffer (4% BSA; Sigma-Aldrich), 10% normal goat serum (Vector Laboratories) overnight at 4°C, monoclonal anti–β-tubulin clone TUB2.1 (Sigma-Aldrich) for 1 h at RT, AlexaFluor488 goat anti–mouse IgG (Invitrogen) for 1 h at RT, and in a 1:5,000 dilution of 1 mg/ml DAPI (Roche) for 20 min at RT before mounting in Vectashield Mounting Medium (Vector Laboratories) on Shandon Multi-Spot microscope slides (Thermo Savant).

Karyotyping

Metaphase spreads of spermatocytes were prepared by the Evans method from the testes of 3-wk-old mutant and control males (Evans et al., 1964). Oocytes were karyotyped by an air-drying method as described previously (Tarkowski, 1966). In brief, mutant and control females were injected with PMS followed by hCG as described above (see Superovulation and collection of oocytes and embryos), and, 14 h later, oocytes arrested at metaphase II were collected from the ampullae in Weimouth media containing penicillin-streptomycin, 10% FBS, and 2.5 mg/ml sodium pyruvate. Chromosome spreads were prepared from the oocytes after a 2-min incubation in 0.9% sodium citrate solution.

HJ resolution assay

Protein extraction was performed as follows: exponentially growing MEFs were collected from ~20 15-cm tissue culture dishes after trypsinization. Approximately 1 g of a cell pellet was resuspended in prechilled lysis buffer (10 mM Tris, pH 8.0, 1 M KCl, 1 mM EDTA, and 1 mM DTT) in the presence of complete EDTA-free protease inhibitor cocktail (Roche). Cells were homogenized by sonication followed by incubation on ice for 1 h. The insoluble pellet was removed by centrifugation at 13,000 rpm for 1 h. Solid $(NH_4)_2SO_4$ (25%; 134 g/liter) was added to the supernatant and dissolved by gentle stirring on ice for 30 min. Insoluble materials were removed by low speed centrifugation (30 min at 9,000 rpm). The $(NH_4)_2SO_4$ concentration was then raised to 55% (an additional 179 g/liter), and the proteins were precipitated during 30 min of stirring on ice. The precipitate was recovered by centrifugation and resuspended in buffer A1 (50 mM K_2HPO_4/KH_2PO_4, pH 6.8, 10% glycerol, 1 mM EDTA, 1 mM DTT, and 0.01% NP-40) containing 250 mM KCl and was dialyzed against the same buffer for 2 h before storage at −80C.

The resolvase assay was performed as follows: for each 10-μl reaction, 1 μl of extract containing 0.9, 1.8, and 3.5 μg of protein was assayed on 1 ng 5′-[^{32}P]end-labeled synthetic HJ DNA (X0) in phosphate buffer (60 mM Na_2HPO_4/NaH_2PO_4, pH 7.4, 5 mM $MgCl_2$, 1 mM DTT, and 100 μg/ml BSA) in the presence of 200 ng of competitor poly[dI:dC] DNA. Incubation was performed for 30 min at 37°C. Products were deproteinized and analyzed by native 10% PAGE. The percentage of resolution was quantified by a phosphoimager (Typhoon 9400 Scanner; Molecular Dynamics).

Online supplemental material

Fig. S1 shows aberrant splicing of the *Rad51c* transcript as a result of the presence of the *PGK-neo* cassette. Fig. S2 shows quantitative analysis of MLH1 foci formation in spermatocytes from control and infertile *Rad51c*$^{ko/neo}$ mice. Figs. S3 and S4 show quantitative analysis of RPA foci (Fig. S3) and RAD51 foci (Fig. S4) in spermatocytes from control and infertile *Rad51c*$^{ko/neo}$ mice. Fig. S5 shows chromosomes from control and *Rad51c*$^{ko/neo}$ oocytes at metaphase I hybridized with a pancentromeric probe as well as sister chromatid cohesion and other defects at metaphase II. Online supplemental material is available at http://www.jcb.org/cgi/content/full/jcb.200608130/DC1.

We thank Drs. Jairaj Acharya, Patricia Hunt, and Philipp Kaldis for helpful discussions and critical review of the manuscript; Dr. Mary Ann Handel for a protocol for metaphase I chromosome preparation from spermatocytes; Martha Susiarjo and Aaron Batterbee for providing valuable technical guidance; Amy Gueye and Chistopher Leasure for technical help; Drs. Peter Moens and Ekaterina Revenkova for antibodies; Keith Rogers and his group in the Histotechnology Laboratory for excellent technical assistance; and Allen Kane of the Publication Department for illustrations.

This research was supported by the National Cancer Institute and the Department of Health and Human Services (grant to A. Nussenzweig, L. Tessarollo, and S.K. Sharan).

Submitted: 22 August 2006
Accepted: 24 January 2007

References

Abdu, U., A. Gonzalez-Reyes, A. Ghabrial, and T. Schupbach. 2003. The *Drosophila* spn-D gene encodes a RAD51C-like protein that is required exclusively during meiosis. *Genetics*. 165:197–204.

Ashley, T., A.W. Plug, J. Xu, A.J. Solari, G. Reddy, E.I. Golub, and D.C. Ward. 1995. Dynamic changes in Rad51 distribution on chromatin during meiosis in male and female vertebrates. *Chromosoma*. 104:19–28.

Baker, S.M., A.W. Plug, T.A. Prolla, C.E. Bronner, A.C. Harris, X. Yao, D.M. Christie, C. Monell, N. Arnheim, A. Bradley, et al. 1996. Involvement of mouse Mlh1 in DNA mismatch repair and meiotic crossing over. *Nat. Genet.* 13:336–342.

Bennett, B.T., and K.L. Knight. 2005. Cellular localization of human Rad51C and regulation of ubiquitin-mediated proteolysis of Rad51. *J. Cell. Biochem.* 96:1095–1109.

Bernard, P., J.F. Maure, and J.P. Javerzat. 2001. Fission yeast Bub1 is essential in setting up the meiotic pattern of chromosome segregation. *Nat. Cell Biol.* 3:522–526.

Bishop, D.K., D. Park, L. Xu, and N. Kleckner. 1992. DMC1: a meiosis-specific yeast homolog of *E. coli* recA required for recombination, synaptonemal complex formation, and cell cycle progression. *Cell*. 69:439–456.

Bleuyard, J.Y., M.E. Gallego, F. Savigny, and C.I. White. 2005. Differing requirements for the *Arabidopsis* Rad51 paralogs in meiosis and DNA repair. *Plant J.* 41:533–545.

Boddy, M.N., P.H. Gaillard, W.H. McDonald, P. Shanahan, J.R. Yates III, and P. Russell. 2001. Mus81-Eme1 are essential components of a Holliday junction resolvase. *Cell*. 107:537–548.

Borum, K. 1961. Oogenesis in the mouse. A study of the meiotic prophase. *Exp. Cell Res.* 24:495–507.

Counce, S.J., and G.F. Meyer. 1973. Differentiation of the synaptonemal complex and the kinetochore in Locusta spermatocytes studied by whole mount electron microscopy. *Chromosoma*. 44:231–253.

Deans, B., C.S. Griffin, M. Maconochie, and J. Thacker. 2000. Xrcc2 is required for genetic stability, embryonic neurogenesis and viability in mice. *EMBO J.* 19:6675–6685.

Dendouga, N., H. Gao, D. Moechars, M. Janicot, J. Vialard, and C.H. McGowan. 2005. Disruption of murine Mus81 increases genomic instability and DNA damage sensitivity but does not promote tumorigenesis. *Mol. Cell. Biol.* 25:7569–7579.

Dobson, M.J., R.E. Pearlman, A. Karaiskakis, B. Spyropoulos, and P.B. Moens. 1994. Synaptonemal complex proteins: occurrence, epitope mapping and chromosome disjunction. *J. Cell Sci.* 107:2749–2760.

Dosanjh, M.K., D.W. Collins, W. Fan, G.G. Lennon, J.S. Albala, Z. Shen, and D. Schild. 1998. Isolation and characterization of RAD51C, a new human member of the RAD51 family of related genes. *Nucleic Acids Res.* 26:1179–1184.

Eaker, S., A. Pyle, J. Cobb, and M.A. Handel. 2001. Evidence for meiotic spindle checkpoint from analysis of spermatocytes from Robertsonian-chromosome heterozygous mice. *J. Cell Sci.* 114:2953–2965.

Evans, E.P., G. Breckon, and C.E. Ford. 1964. An air-drying method for meiotic preparations from mammalian testes. *Cytogenetics*. 15:289–294.

Gasior, S.L., H. Olivares, U. Ear, D.M. Hari, R. Weichselbaum, and D.K. Bishop. 2001. Assembly of RecA-like recombinases: distinct roles for mediator proteins in mitosis and meiosis. *Proc. Natl. Acad. Sci. USA*. 98:8411–8418.

Godthelp, B.C., W.W. Wiegant, A. van Duijn-Goedhart, O.D. Scharer, P.P. van Buul, R. Kanaar, and M.Z. Zdzienicka. 2002. Mammalian Rad51C

contributes to DNA cross-link resistance, sister chromatid cohesion and genomic stability. *Nucleic Acids Res.* 30:2172–2182.

Hodges, C.A., R. LeMaire-Adkins, and P.A. Hunt. 2001. Coordinating the segregation of sister chromatids during the first meiotic division: evidence for sexual dimorphism. *J. Cell Sci.* 114:2417–2426.

Hogan, B., R. Beddington, F. Constantini, and E. Lacy. 1994. Manipulating the Mouse Embryo: a Laboratory Manual. Cold Spring Harbor Laboratory Press, Cold Spring Harbor, NY. 497 pp.

Hunt, P.A., and T.J. Hassold. 2002. Sex matters in meiosis. *Science*. 296:2181–2183.

Indjeian, V.B., B.M. Stern, and A.W. Murray. 2005. The centromeric protein Sgo1 is required to sense lack of tension on mitotic chromosomes. *Science*. 307:130–133.

Kawabata, M., T. Kawabata, and M. Nishibori. 2005. Role of recA/RAD51 family proteins in mammals. *Acta Med. Okayama*. 59:1–9.

Kitajima, T.S., S.A. Kawashima, and Y. Watanabe. 2004. The conserved kinetochore protein shugoshin protects centromeric cohesion during meiosis. *Nature*. 427:510–517.

Koehler, K.E., E.A. Millie, J.P. Cherry, P.S. Burgoyne, E.P. Evans, P.A. Hunt, and T.J. Hassold. 2002. Sex-specific differences in meiotic chromosome segregation revealed by dicentric bridge resolution in mice. *Genetics*. 162:1367–1379.

Leasure, C.S., J. Chandler, D.J. Gilbert, D.B. Householder, R. Stephens, N.G. Copeland, N.A. Jenkins, and S.K. Sharan. 2001. Sequence, chromosomal location and expression analysis of the murine homologue of human RAD51L2/RAD51C. *Gene*. 271:59–67.

Lewandoski, M., E.N. Meyers, and G.R. Martin. 1997. Analysis of Fgf8 gene function in vertebrate development. *Cold Spring Harb. Symp. Quant. Biol.* 62:159–168.

Li, W., X. Yang, Z. Lin, L. Timofejeva, R. Xiao, C.A. Makaroff, and H. Ma. 2005. The AtRAD51C gene is required for normal meiotic chromosome synapsis and double-stranded break repair in *Arabidopsis*. *Plant Physiol*. 138:965–976.

Libby, B.J., R. De La Fuente, M.J. O'Brien, K. Wigglesworth, J. Cobb, A. Inselman, S. Eaker, M.A. Handel, J.J. Eppig, and J.C. Schimenti. 2002. The mouse meiotic mutation mei1 disrupts chromosome synapsis with sexually dimorphic consequences for meiotic progression. *Dev. Biol.* 242:174–187.

Lio, Y.C., D. Schild, M.A. Brenneman, J.L. Redpath, and D.J. Chen. 2004. Human Rad51C deficiency destabilizes XRCC3, impairs recombination, and radiosensitizes S/G2-phase cells. *J. Biol. Chem.* 279:42313–42320.

Liu, Y., J.Y. Masson, R. Shah, P. O'Regan, and S.C. West. 2004. RAD51C is required for Holliday junction processing in mammalian cells. *Science*. 303:243–246.

Liu, Y., M. Tarsounas, P. O'Regan, and S.C. West. 2007. Role of RAD51C and XRCC3 in genetic recombination and DNA repair. *J. Biol. Chem*. 282:1973–1979.

Mahadevaiah, S.K., E.P. Evans, and P.S. Burgoyne. 2000. An analysis of meiotic impairment and of sex chromosome associations throughout meiosis in XYY mice. *Cytogenet. Cell Genet.* 89:29–37.

Mahadevaiah, S.K., J.M. Turner, F. Baudat, E.P. Rogakou, P. de Boer, J. Blanco-Rodriguez, M. Jasin, S. Keeney, W.M. Bonner, and P.S. Burgoyne. 2001. Recombinational DNA double-strand breaks in mice precede synapsis. *Nat. Genet.* 27:271–276.

Mailhes, J.B., M.J. Carabatsos, D. Young, S.N. London, M. Bell, and D.F. Albertini. 1999. Taxol-induced meiotic maturation delay, spindle defects, and aneuploidy in mouse oocytes and zygotes. *Mutat. Res.* 423:79–90.

Masson, J.Y., M.C. Tarsounas, A.Z. Stasiak, A. Stasiak, R. Shah, M.J. McIlwraith, F.E. Benson, and S.C. West. 2001. Identification and purification of two distinct complexes containing the five RAD51 paralogs. *Genes Dev.* 15:3296–3307.

Meyers, E.N., M. Lewandoski, and G.R. Martin. 1998. An Fgf8 mutant allelic series generated by Cre- and Flp-mediated recombination. *Nat. Genet.* 18:136–141.

Miller, K.A., D. Sawicka, D. Barsky, and J.S. Albala. 2004. Domain mapping of the Rad51 paralog protein complexes. *Nucleic Acids Res.* 32:169–178.

Pittman, D.L., and J.C. Schimenti. 2000. Midgestation lethality in mice deficient for the RecA-related gene, Rad51d/Rad51l3. *Genesis*. 26:167–173.

Plug, A.W., A.H. Peters, Y. Xu, K.S. Keegan, M.F. Hoekstra, D. Baltimore, P. de Boer, and T. Ashley. 1997. ATM and RPA in meiotic chromosome synapsis and recombination. *Nat. Genet.* 17:457–461.

Prieto, I., C. Tease, N. Pezzi, J.M. Buesa, S. Ortega, L. Kremer, A. Martinez, A.C. Martinez, M.A. Hulten, and J.L. Barbero. 2004. Cohesin component dynamics during meiotic prophase I in mammalian oocytes. *Chromosome Res.* 12:197–213.

Revenkova, E., M. Eijpe, C. Heyting, C.A. Hodges, P.A. Hunt, B. Liebe, H. Scherthan, and R. Jessberger. 2004. Cohesin SMC1 beta is required for meiotic chromosome dynamics, sister chromatid cohesion and DNA recombination. *Nat. Cell Biol.* 6:555–562.

Riedel, C.G., V.L. Katis, Y. Katou, S. Mori, T. Itoh, W. Helmhart, M. Galova, M. Petronczki, J. Gregan, B. Cetin, et al. 2006. Protein phosphatase 2A protects centromeric sister chromatid cohesion during meiosis I. *Nature*. 441:53–61.

Rodrigue, A., M. Lafrance, M.C. Gauthier, D. McDonald, M. Hendzel, S.C. West, M. Jasin, and J.Y. Masson. 2006. Interplay between human DNA repair proteins at a unique double-strand break in vivo. *EMBO J.* 25:222–231.

Romanienko, P.J., and R.D. Camerini-Otero. 2000. The mouse Spo11 gene is required for meiotic chromosome synapsis. *Mol. Cell*. 6:975–987.

Schwacha, A., and N. Kleckner. 1997. Interhomolog bias during meiotic recombination: meiotic functions promote a highly differentiated interhomolog-only pathway. *Cell*. 90:1123–1135.

Sharan, S.K., A. Pyle, V. Coppola, J. Babus, S. Swaminathan, J. Benedict, D. Swing, B.K. Martin, L. Tessarollo, J.P. Evans, et al. 2004. BRCA2 deficiency in mice leads to meiotic impairment and infertility. *Development*. 131:131–142.

Shu, Z., S. Smith, L. Wang, M.C. Rice, and E.B. Kmiec. 1999. Disruption of muREC2/RAD51L1 in mice results in early embryonic lethality which can be partially rescued in a p53(−/−) background. *Mol. Cell. Biol.* 19:8686–8693.

Sigurdsson, S., S. Van Komen, W. Bussen, D. Schild, J.S. Albala, and P. Sung. 2001. Mediator function of the human Rad51B-Rad51C complex in Rad51/RPA-catalyzed DNA strand exchange. *Genes Dev.* 15:3308–3318.

Sung, P. 1997. Yeast Rad55 and Rad57 proteins form a heterodimer that functions with replication protein A to promote DNA strand exchange by Rad51 recombinase. *Genes Dev.* 11:1111–1121.

Szostak, J.W., T.L. Orr-Weaver, R.J. Rothstein, and F.W. Stahl. 1983. The double-strand-break repair model for recombination. *Cell*. 33:25–35.

Takata, M., M.S. Sasaki, S. Tachiiri, T. Fukushima, E. Sonoda, D. Schild, L.H. Thompson, and S. Takeda. 2001. Chromosome instability and defective recombinational repair in knockout mutants of the five Rad51 paralogs. *Mol. Cell. Biol.* 21:2858–2866.

Tarkowski, A.K. 1966. An air-drying method for chromosome preparations from mouse eggs. *Cytogenetics*. 5:394–400.

Tarsounas, M., P. Munoz, A. Claas, P.G. Smiraldo, D.L. Pittman, M.A. Blasco, and S.C. West. 2004. Telomere maintenance requires the RAD51D recombination/repair protein. *Cell*. 117:337–347.

Vaur, S., F. Cubizolles, G. Plane, S. Genier, P.K. Rabitsch, J. Gregan, K. Nasmyth, V. Vanoosthuyse, K.G. Hardwick, and J.P. Javerzat. 2005. Control of Shugoshin function during fission-yeast meiosis. *Curr. Biol.* 15:2263–2270.

Wang, X., and W. Dai. 2005. Shugoshin, a guardian for sister chromatid segregation. *Exp. Cell Res.* 310:1–9.

Woods, L.M., C.A. Hodges, E. Baart, S.M. Baker, M. Liskay, and P.A. Hunt. 1999. Chromosomal influence on meiotic spindle assembly: abnormal meiosis I in female Mlh1 mutant mice. *J. Cell Biol.* 145:1395–1406.

Xu, H., M.D. Beasley, W.D. Warren, G.T. van der Horst, and M.J. McKay. 2005. Absence of mouse REC8 cohesin promotes synapsis of sister chromatids in meiosis. *Dev. Cell*. 8:949–961.

Yin, H., E. Baart, I. Betzendahl, and U. Eichenlaub-Ritter. 1998. Diazepam induces meiotic delay, aneuploidy and predivision of homologues and chromatids in mammalian oocytes. *Mutagenesis*. 13:567–580.

Yonetani, Y., H. Hochegger, E. Sonoda, S. Shinya, H. Yoshikawa, S. Takeda, and M. Yamazoe. 2005. Differential and collaborative actions of Rad51 paralog proteins in cellular response to DNA damage. *Nucleic Acids Res.* 33:4544–4552.

Yuan, L., J.G. Liu, M.R. Hoja, J. Wilbertz, K. Nordqvist, and C. Hoog. 2002. Female germ cell aneuploidy and embryo death in mice lacking the meiosis-specific protein SCP3. *Science*. 296:1115–1118.